Chemical Science

ROYAL SOCIETY OF CHEMISTRY

EDGE ARTICLE

View Article Online
View Journal | View Issue

Check for updates

Cite this: *Chem. Sci.*, 2024, **15**, 5653

All publication charges for this article have been paid for by the Royal Society of Chemistry

Received 18th January 2024
Accepted 10th March 2024

DOI: 10.1039/d4sc00424h

rsc.li/chemical-science

A novel hydrophobic carborane-hybrid microporous material for reversed C_2H_6 adsorption and efficient C_2H_4/C_2H_6 separation under humid conditions†

Lingyao Wang,‡[a] Shuangshuang Wu,‡[a] Jianbo Hu,‡[b] Yunjia Jiang,[a] Jiahao Li,[a] Yongqi Hu,[a] Yan Han,[a] Teng Ben,[c] Banglin Chen[ad] and Yuanbin Zhang*[a]

Since ethylene (C_2H_4) is important feedstock in the chemical industry, developing economical and energy-efficient adsorption separation techniques based on ethane (C_2H_6)-selective adsorbents to replace the energy-intensive cryogenic distillation is highly demanded, which however remains a daunting challenge. While previous anionic boron cluster hybrid microporous materials display C_2H_4-selective features, we herein reported that the incorporation of a neutral *para*-carborane backbone and aliphatic 1,4-diazabicyclo[2.2.2]octane (DABCO) enables the reversed adsorption of C_2H_6 over C_2H_4. The generated carborane-hybrid microporous material ZNU-10 (ZNU = Zhejiang Normal University) is highly stable in humid air and maintains good C_2H_6/C_2H_4 separation performance under high humidity. Gas loaded single crystal structure and density-functional theory (DFT) calculations revealed that the weakly polarized carborane and DABCO within ZNU-10 induce more specific $C{-}H^{\delta+}\cdots H^{\delta-}{-}B$ dihydrogen bonds and other van der Waals interactions with C_2H_6, while the suitable pore space allows the high C_2H_6 uptake. Approximately 14.5 L kg^{-1} of polymer grade C_2H_4 can be produced from simulated C_2H_6/C_2H_4 (v/v 10/90) mixtures under ambient conditions in a single step, comparable to those of many popular materials.

Introduction

Polymer-grade ethylene ($C_2H_4 > 99.9\%$) is significant feedstock to produce resins and plastics.[1] During the production, ethane (C_2H_6) is the major impurity and needs to be removed to improve the C_2H_4 quality. The current state-of-the-art technique to separate C_2H_4/C_2H_6 depends on cryogenic distillation at high pressure and low temperature.[2] The separation process is highly energy-intensive due to the similarity of the boiling points of C_2H_4 (−88.6 °C) and C_2H_6 (−103.7 °C) and requires very large distillation towers with 120 to 180 trays and high reflux ratios.[3] Therefore, there is a need to develop novel technologies for efficient C_2H_4/C_2H_6 separation.[4]

Recently, physisorptive separation using porous solid adsorbents has attracted increasing attention due to its environmental friendliness and reduced energy consumption.[5] Porous coordination polymers (PCPs) or metal–organic frameworks (MOFs), as a new class of crystalline porous materials with a high surface area, structural tailorability and controllable properties, have been developed for the separation of C_2H_4/C_2H_6 hydrocarbon mixtures.[6] Among them, most MOF materials, especially those decorated with polar functional groups or unsaturated metal sites, exhibit the preferential adsorption order of $C_2H_4 > C_2H_6$ based on their difference in physicochemical properties including molecular size, polarity and quadrupole moment (Table S2†).[7] However, C_2H_4-selective MOFs are not the optimal selection for the adsorptive separation of C_2H_4/C_2H_6 mixtures. The concentration of C_2H_4 within the cracked gas mixtures is often over 10 times higher than that of C_2H_6, thus using C_2H_4-selective adsorbents for C_2H_4/C_2H_6 separation entails more adsorbent consumption and larger space occupation than using C_2H_6-selective adsorbents.[8] Besides, the utilization of C_2H_4-selective adsorbents usually needs over four adsorption–desorption cycles to attain polymer-grade C_2H_4 due to the retention of C_2H_6 amidst adsorbent

---

[a] *Key Laboratory of the Ministry of Education for Advanced Catalysis Materials, College of Chemistry and Materials Science, Zhejiang Normal University, Jinhua, 321004, China. E-mail: ybzhang@zjnu.edu.cn*

[b] *Zhejiang Lab, Hangzhou, 311100, P. R. China*

[c] *Institute of Advanced Fluorine-Containing Materials, Zhejiang Normal University, Jinhua, 321004, China*

[d] *Fujian Provincial Key Laboratory of Polymer Materials, College of Chemistry & Materials Science, Fujian Normal University, Fuzhou, 350007, P. R. China*

† Electronic supplementary information (ESI) available. CCDC 2287884, 2287885, 2287887 and 2287888. For ESI and crystallographic data in CIF or other electronic format see DOI: **https://doi.org/10.1039/d4sc00424h**

‡ These authors contributed equally to this work.

particles.[9] In sharp contrast, using C_2H_6-selective adsorbents facilitates the direct acquisition of high-purity C_2H_4 through a single adsorption step, streamlining the separation process and effecting approximately a 40% reduction in energy consumption.[10] Hence, the development of C_2H_6-selective adsorbents is highly imperative for industrial refinement of C_2H_4. In previous reports, reducing the polarity of pore surfaces in porous materials is promising to afford reversed adsorption of C_2H_6 over C_2H_4.[11] This phenomenon can be regarded as "like adsorbs like" when compared to the "like dissolves like" principle. However, the construction of C_2H_6-selective MOFs is still a difficult problem at present.

With the above consideration in mind, we envision that three dimensional neutral *para*-carborane (p-$C_2B_{10}H_{12}$) as a derivative of the $[B_{12}H_{12}]^{2-}$ anion (Scheme 1) can serve as a weakly polarized functional group in MOFs to selectively bind C_2H_6 over C_2H_4. Although a plenty of dodecaborate $[B_{12}H_{12}]^{2-}$ anion pillared MOFs have been developed in our group for gas separation with efficient C_2H_2/CO_2 and C_2H_2/C_2H_4 splitting performance,[12] carborane-based MOFs have been rarely reported,[13] and no records of light hydrocarbon separation with carborane hybrid MOFs can be traced. On the other hand, carborane hybrid MOFs seem to display higher water stability when compared to benzene-based MOF analogues, which is a benefit for real applications with moisture.[13a,d]

Herein, we reported a novel microporous MOF termed ZNU-10 (ZNU = Zhejiang Normal University) with cluster *para*-carboranyl dicarboxylic acid (1,12-p-$C_2B_{10}H_{10}$-$(COOH)_2$) and 1,4-diazobicyclo[2.2.2]octane (DABCO) as the backbones. A pillar-layered framework with pcu topology and saturated metal sites is generated when assembled with classical paddle-wheel dicopper(II) SBUs. As a result, these pores with uniform electrostatic potential not only help to reverse the adsorption sequence of C_2H_6 over C_2H_4, but also contribute to improving the water stability of the framework due to the hydrophobic surface of the pore channel. Despite its higher affinity towards C_2H_6, the C_2H_6 adsorption heat (26.4 kJ mol^{-1}) in ZNU-10 is quite low, allowing its facile regeneration. *In situ* gas loaded single crystal structures and density-functional theory (DFT) calculations were applied to reveal the adsorption mechanism. In the poorly polarized channels, C_2H_6 molecules are stacked more closely and feature stronger van der Waals interactions and $C\text{–}H^{\delta+}\cdots H^{\delta-}\text{–}B$ dihydrogen bonding to the framework due to the larger molecular size and polarizability. Experimental breakthrough studies confirmed that one-step acquisition of high-purity C_2H_4 from C_2H_4/C_2H_6 mixtures can be realized with a high production of *ca.* 14.5 L kg^{-1}.

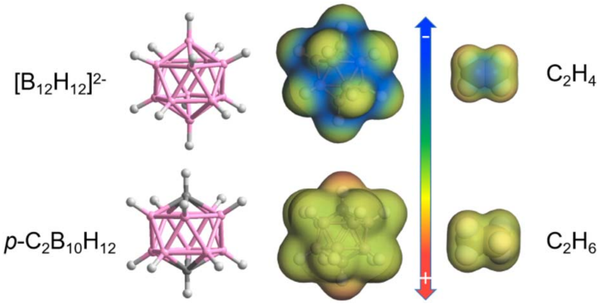

Scheme 1 Comparison of the surface electrostatic potential of boron clusters (dodecaborate dianion and p-carborane) and C_2 hydrocarbon gases (C_2H_6/C_2H_4).

Results and discussion

Greenish-blue single crystals of ZNU-10 {Cu(1,12-p-$C_2B_{10}H_{10}$-$(COO)_2$)$(DABCO)_{0.5}$} were produced by a solvothermal reaction of $Cu(NO_3)_2\cdot 3H_2O$, p-$C_2B_{10}H_{10}$-$(COOH)_2$ and DABCO in a mixed DMF/MeOH/H_2O (v/v/v = 2/2/1) solution (Fig. S1†). Single crystal X-ray diffraction (SCXRD) analysis showed that $Cu_2(COO)_4$ paddle wheel secondary building units (SBUs) are formed between two Cu^{2+} and four carboxylate ligands (Fig. 1A). Each SBU paddle wheel is connected by p-carborane ligands to form a two-dimensional (2D) square grid layer (Fig. 1B). The layers are further pillared by the organic DABCO ligands to generate a 3D framework with pcu topology and saturated metal sites (Fig. 1C). The analysis of the surface electrostatic potential of ZNU-10 indicates that ZNU-10 features a uniform and poorly polarized pore surface (Fig. 1D). This is because ZNU-10 consists of a neutral carborane backbone and aliphatic organic building blocks. When compared, ZNU-1 {$CuB_{12}H_{12}$(-dpe)$_2$}[12a] constructed from −2 charged $[B_{12}H_{12}]^{2-}$ backbones and aromatic ligands displays similar 1D channels but significantly different electrostatic potential on the pore surface. Notable charge separation can be observed on the isosurface of ZNU-1, namely the anionic boron cluster surface displays highly negative electrostatic potential while the organic linker surface displays very positive electrostatic potential (Fig. 1F). As we know, ZNU-1 is one of the best MOFs to selectively capture C_2H_2 from various mixtures.[12a,b] Due to the completely different electrostatic potential distribution, ZNU-10 is yet supposed to be a C_2H_6 selective adsorbent for one-step C_2H_4 acquisition from C_2H_4/C_2H_6 mixtures.

Before gas adsorption experiments, we investigated the chemical and thermal stability of ZNU-10 to optimize the activation conditions. We find that ZNU-10 is highly stable in many organic solvents including DMA, EtOH, *n*-hexane, acetone, CH_2Cl_2, DMF, MeCN, MeOH and so on, identified by a microphotograph (Fig. 2A) and powder X-ray diffraction (PXRD) (Fig. 2B). Temperature varied PXRD and thermogravimetric analysis (TGA) indicated that ZNU-10 is stable below 320 °C (Fig. 2C and D). Such thermal stability is superior to that of all the boron cluster anion hybrid MOFs and most Cu(II) based MOFs (Fig. S10 and S11†).[12] According to the above results, the as-synthesized ZNU-10 was soaked in MeOH for solvent-exchange and activated under 120 °C to fully remove all the guest molecules. Besides, we find that ZNU-10 is highly stable in humid air. The as-synthesized single crystals retained the crystallinity and quality over 3 months under an ambient humid atmosphere or heating at 120 °C for 3 days under vacuum (Fig. 3D, inset), identified by single crystal X-ray analysis.

The permanent porosity of ZNU-10 was established by N_2 gas adsorption experiments at 77 K. The adsorption isotherm corresponds to the representative type I adsorption isotherm,

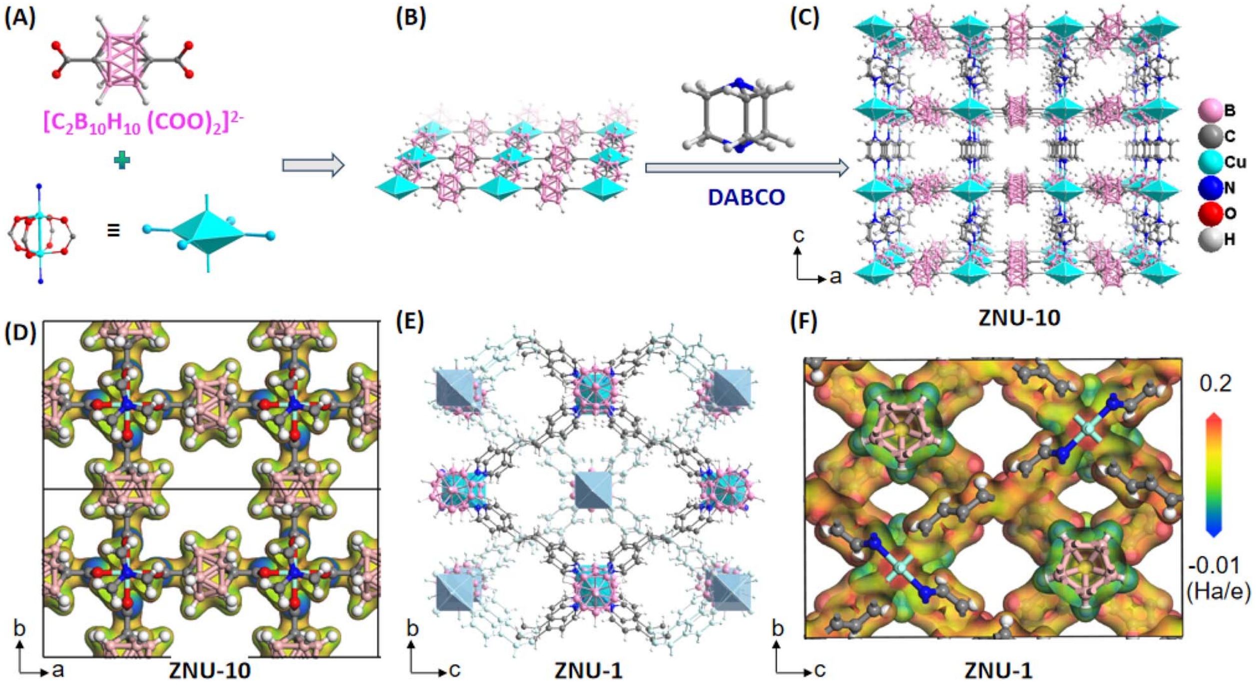

Fig. 1 (A and B) Single layer of ZNU-10 constructed from carborane dicarboxylic acid and Cu(II) paddle wheels. (C) 3D structure of ZNU-10 viewed along the *b* axis. (D) Isosurface of ZNU-10 viewed along the *c* axis. (E) Structure of ZNU-1 viewed along the *a* axis. (F) Isosurface of ZNU-1 viewed along the *a* axis.

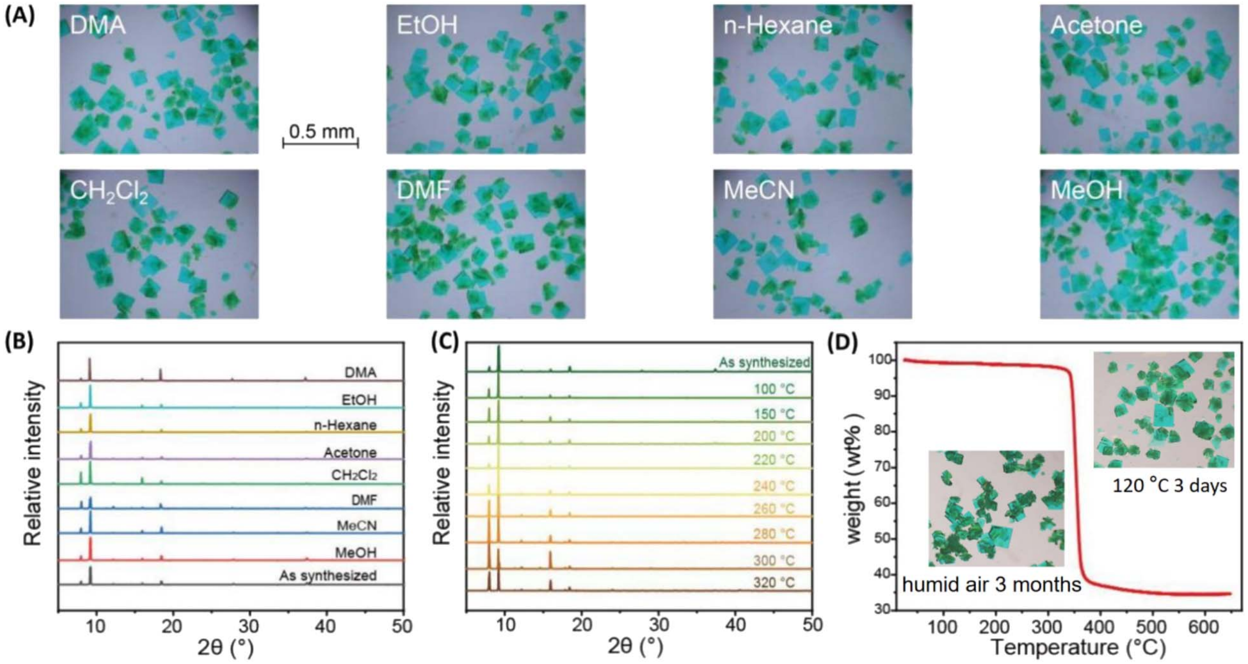

Fig. 2 (A) Microphotograph of single crystals and (B) PXRD of ZNU-10 after soaking in different solvents for 3 months. (C) Temperature varied PXRD of ZNU-10. (D) TGA curve of ZNU-10 (inset: microphotograph of single crystals of ZNU-10 after heating at 120 °C for 3 days or exposure to humid air for 3 months).

indicative of its inherent microporous characteristics (Fig. 3A). At $P/P_0 = 0.95$, the N_2 adsorption capacity of ZNU-10 was 293 STP $cm^3\ g^{-1}$ (13.1 mmol g^{-1}), and the Brunauer–Emmett–Teller (BET) surface area and micropore volume are calculated to be 1171 $m^2\ g^{-1}$ and 0.45 $cm^3\ g^{-1}$, respectively. The calculated pore size is centered at 8.59 Å (Fig. S13†), which is very close to the

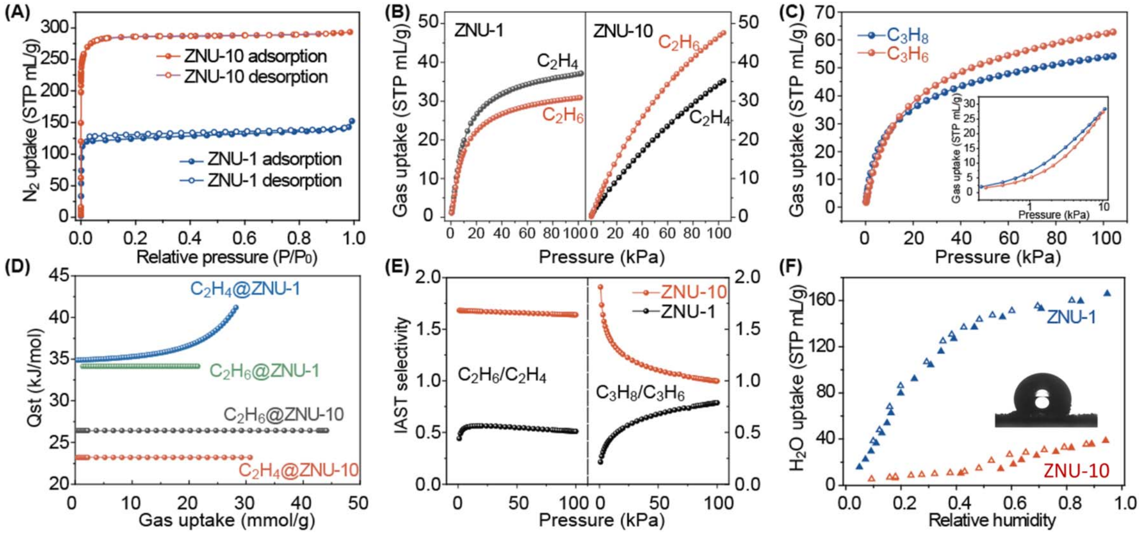

Fig. 3 (A) N_2 sorption isotherms for ZNU-1 and ZNU-10 at 77 K. (B) C_2H_4 and C_2H_6 adsorption isotherms for ZNU-10 at 298 K. (C) C_3H_6 and C_3H_8 adsorption isotherms for ZNU-10 at 298 K (inset: adsorption isotherms in the pressure region of 0–10 kPa). (D) The isosteric heat of adsorption (Q_{st}) of C_2H_4 and C_2H_6 for ZNU-10 and ZNU-1. (E) IAST selectivity of equimolar C_2H_6/C_2H_4 and C_3H_8/C_3H_6 at 298 K. (F) Water sorption isotherms for ZNU-10 and ZNU-1 at 298 K (inset: contact angle testing of ZNU-10).

pore size of 7.7–10 Å from the single crystal structure evaluation (Fig. S6 and S7†). When compared, ZNU-1 only displays a BET surface area of 532 $m^2\ g^{-1}$ and a pore volume of 0.20 $cm^3\ g^{-1}$ (Fig. S14†). Therefore, the porosity of ZNU-10 (Fig. S4 and S5†) is significantly increased when compared to that of ZNU-1.

Single component C_2H_6 and C_2H_4 adsorption measurements at 298 K were conducted for ZNU-10 and ZNU-1. At 1.0 bar, the C_2H_6 and C_2H_4 uptakes on ZNU-10 were 47.6 and 35.1 STP $cm^3\ g^{-1}$ (2.13 and 1.57 mmol g^{-1}), respectively (Fig. 3B, right). This uptake trend is opposite to that of ZNU-1 (30.9 and 37.1 STP $cm^3\ g^{-1}$ for C_2H_6 and C_2H_4) (Fig. 3B, left). With the temperature decreasing to 278 K, the C_2H_6 and C_2H_4 uptakes on ZNU-10 were improved to 67.9 and 55.1 $cm^3\ g^{-1}$ (Fig. S17 and S18†). The reversed adsorption of C_3H_8 and C_3H_6 is also observed in the low pressure region for ZNU-10 (Fig. 3C), which is quite rare in MOFs.[14]

In order to quantitatively compare the adsorption affinity between the framework and gas molecules, we calculated the adsorption heats (Q_{st}) of ZNU-10 and ZNU-1 using the Clausius–Clapeyron equation after fitting the isotherms to Langmuir equations with excellent accuracy (Tables S3 and S4†). The Q_{st} values of C_2H_6 and C_2H_4 for ZNU-10 were 26.4 and 23.2 kJ mol^{-1}, respectively; while those for ZNU-1 were 34.1 and 34.9 kJ mol^{-1}, respectively (Fig. 3D). These Q_{st} values are consistent with the slope of the adsorption isotherms in the low pressure region. Notably, the C_2H_6 adsorption heat on ZNU-10 is much lower than those in most C_2H_6-selective materials such as $Fe_2(O_2)$(dobdc) (67 kJ mol^{-1}),[15] MAF-49 (60 kJ mol^{-1}),[16] UiO-NDC (58 kJ mol^{-1}),[17] NKMOF-8-Br (40.8 kJ mol^{-1})[18] and FJI-H11-Me (38.9 kJ mol^{-1}),[19] and even lower than that of C_2H_6-disfavored ZNU-1. This extremely low adsorption heat allows the facile regeneration of ZNU-10 for recyclable use.

The separation selectivity of C_2H_6/C_2H_4 is further calculated based on ideal adsorption solution theory (IAST). The C_2H_6/C_2H_4 selectivity on ZNU-10 is 1.68∼1.64 in the range of 1–100 kPa (Fig. 3E), which is approximately 3.2 times that of ZNU-1 ($S = 0.51$ at 100 kPa). This C_2H_6/C_2H_4 selectivity is also higher than those of many C_2H_6 selective MOFs such as UiO-NDC (1.35),[17] UPC-612 (1.4),[20] TJT-100 (1.2),[21] LIFM-63 (1.56),[22] JNU-2 (1.6)[23] and Azole-Th-1 (1.46).[24] Besides, the C_2H_6/C_2H_4 selectivity on ZNU-10 remains consistent regardless of the C_2H_6/C_2H_4 ratio (Fig. S22†). The equimolar C_3H_8/C_3H_6 selectivity for ZNU-10 and ZNU-1 from 1 to 100 kPa is calculated to be 1.91–1.00 and 0.21–0.78, respectively, further indicating the opposite affinity of ZNU-10 and ZNU-1 towards olefins and paraffins.

To further explore the pore difference of ZNU-10 and ZNU-1, we performed a water vapor adsorption test. The results showed that at a relative humidity of 0.9, the water vapor adsorption capacity of ZNU-10 was only 35.6 mL g^{-1}, much lower than that of ZNU-1 (*ca.* 162 mL g^{-1}) under the same conditions (Fig. 3F). These results showed that ZNU-10 is more hydrophobic and has high potential to remove the C_2H_6 impurity from C_2H_4/C_2H_6 mixtures under humid environmental conditions. The water stability is also confirmed by soaking the ZNU-10 crystals in water. Initially, ZNU-10 floated on the surface of water due to its low density (0.933 $cm^3\ g^{-1}$) and hydrophobicity. After some time, ZNU-10 crystals sunk to the bottom of water and became blue powders slowly. Nonetheless, the PXRD pattern of the water-soaked ZNU-10 is still consistent with that of the as-synthesized one (Fig. S25†). We also measured the water contact angle of ZNU-10, and the large water contact angle of >114° also indicated the hydrophobic nature of ZNU-10 (Fig. S26†).

Due to the high stability of ZNU-10 single crystals, the *in situ* single crystal structure of ZNU-10 with the loading of C_2H_6 or C_2H_4 was studied. We found that on average 0.7 C_2H_6 and 0.55 C_2H_4 molecules are adsorbed by a carborane unit (Fig. 4A and B), which corresponds to *ca.* 45 and 35 STP $cm^3\ g^{-1}$ of C_2H_6 and

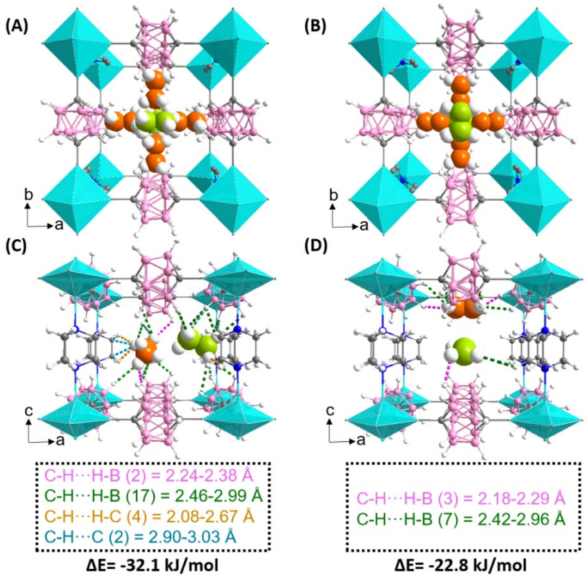

Fig. 4 (A and B) *In situ* single crystal structure of C_2H_6@ZNU-10 and C_2H_4@ZNU-10 viewed along the *c* axis. (C and D) DFT calculated C_2H_6 and C_2H_4 adsorption configuration in ZNU-10 viewed along the *b* axis and the corresponding binding energies.

C_2H_4, respectively. These uptake values are close to the gas uptake from the adsorption isotherms at 1.0 bar. For both gases, two different binding sites are observed. The first site is located close to the window consisting of two carboranes and two DABCO (Fig. S9A and B†). There are four such sites in a single unit cell. The second site is located close to the window consisting of four carboranes (Fig. S9C and D†). There are two such sites in every unit cell. Therefore, six gas molecules can be adsorbed in a unit cell at maximum. However, the single crystal structure analysis indicated that the occupancy of gas molecules at each position is less than one. This could be explained by the low adsorption heats of C_2H_6 and C_2H_4 in ZNU-10 and the high symmetry of the framework. Due to the disorder, the contact distance between the gas molecules and the framework is not precise. Nonetheless, more close van der Waals interactions and C–$H^{\delta+}\cdots H^{\delta-}$–B dihydrogen bonds are observed for C_2H_6 molecules. For example, the closest C–$H^{\delta+}\cdots H^{\delta-}$–B distance between C_2H_6 and ZNU-10 is 2.10 Å, while that for C_2H_4 is 2.32 Å.

To gain more insights into the gas adsorption behavior, modeling studies using DFT calculations were further performed. The calculated average bonding energy between ZNU-10 and two gases located at different sites based on the *in situ* single crystal structures is −32.1 and −22.8 kJ mol^{-1} for C_2H_6 and C_2H_4, respectively (Fig. 4C and D), consistent with the experimental Q_{st} trend. In site I, C_2H_6 interacts with two carborane backbones by multiple C–H⋯H–B interactions. The contact between C_2H_6 and DABCO is also observed, with H⋯H distances of 2.08–2.67 Å and H⋯C distances of 2.90–3.03 Å. In site II, there only exist weak C–H⋯H–B interactions with a distance of >2.4 Å. When compared, C_2H_4 displays slightly shorter contact distances (2.18 and 2.21 Å in site I and 2.29 in site II) but decreased binding energy due to the fact that the overall interactions are fewer. This is consistent with the fact that C_2H_4 has small molecular size and thus the confinement in the nanospace of ZNU-10 will be weaker.

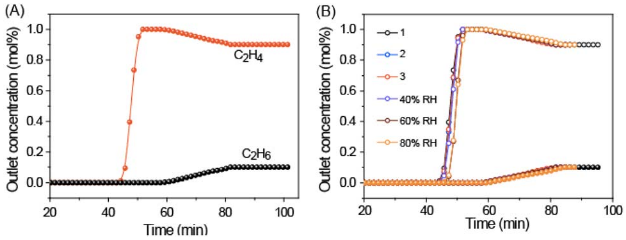

Fig. 5 (A) The column breakthrough curves of ZNU-10 for C_2H_4/C_2H_6 (90/10) mixtures at 298 K. (B) Repeated column breakthrough curves of ZNU-10 for C_2H_4/C_2H_6 (90/10) mixtures under dry and humid conditions.

To evaluate the feasibility of ZNU-10 for practical C_2H_4 purification from binary C_2H_4/C_2H_6 mixtures, lab-scale breakthrough experiments were conducted for the C_2H_4/C_2H_6 (90/10) mixture to simulate the real separation conditions (Fig. S22†). Fig. 5A shows that high-purity C_2H_4 (>99.9%) was obtained between 44 and 58 min. The polymer grade C_2H_4 (>99.9%) productivity is estimated to be as high as 14.5 L kg^{-1} (647 mmol kg^{-1}), superior to those of NKU-301 (9.5 L kg^{-1}),[14] Zr-TCA (6.51 L kg^{-1}),[25] MOF-801 (5.73 L kg^{-1}),[26] UiO-66 (0.46 L kg^{-1})[25] and many other popular materials under the same conditions.[11] Besides, ZNU-10 displays high recyclability and resistance to humidity. The breakthrough time is almost the same for multiple cycles or under highly humid conditions (Fig. 5B). Besides, ZNU-10 can be readily generated under Ar purge at room temperature within 1 h (Fig. S24†), which is consistent with the low adsorption heat of C_2H_6 and C_2H_4 in ZNU-10. The regeneration can also be achieved by desorption under vacuum for 1 h. In brief, the combination of high productivity of pure C_2H_4, good recycling performance and facile regeneration conditions of the material makes ZNU-10 as a potential adsorbent for practical C_2H_4 purification.

Conclusions

In conclusion, we have reported a novel hydrophobic carborane hybrid metal–organic framework ZNU-10 with reversed C_2H_6 adsorption properties for efficient capture of C_2H_6 from C_2H_4/C_2H_6 mixtures to produce high-purity C_2H_4 in a single step. ZNU-10 displays distinct electrostatic potential distribution in the pore surface compared to the analogue cluster boron anion pillared ZNU-1. The difference leads to reversed C_2H_4/C_2H_6 hydrocarbon adsorption orders in ZNU-10 and ZNU-1. Notably, ZNU-10 exhibits good chemical/thermal stability with resistance towards water adsorption due to its hydrophobic pore surface. The excellent C_2H_4/C_2H_6 separation performance is fully illustrated by breakthrough experiments with good recyclability and capacity retention under high humidity. In general, our work demonstrates the versatility and importance of boron cluster functionalities, which can be tuned to achieve desirable gas adsorption properties. Considering the large library of boron cluster compounds, this work will open a new avenue in boron cluster chemistry for light hydrocarbon separation applications.

Data availability

All the data supporting this article have been included in the main text and the ESI.†

Author contributions

L. W.: investigation, structural determination and analysis, funding, and supervision; S. W.: synthesis, characterization, and adsorption experiments; J. H.: DFT calculation; Y. J.: investigation and discussion; J. Li: adsorption experiments; Y. H.: breakthrough experiments; Y. H.: breakthrough experiments; T. B.: supervision; B. C.: supervision and funding; Y. Z.: concept, supervision, draft and funding.

Conflicts of interest

There are no conflicts to declare.

Acknowledgements

This work was supported by the Natural Science Foundation of China (No. 22205207, 22378369 and 22008209), Major project of Natural Science Foundation of Zhejiang Province (LD24B060001) and Jinhua Industrial Key Project (No. 2021-1-088).

References

1 X. Cui, K. Chen, H. Xing, Q. Yang, R. Krishna, Z. Bao, H. Wu, W. Zhou, X. Dong, Y. Han, B. Li, Q. Ren, M. J. Zaworotko and B. Chen, *Science*, 2016, **353**, 141–144.

2 (*a*) D. S. Sholl and R. P. Lively, *Nature*, 2016, **532**, 435–437; (*b*) K. Chen, D. G. Madden, S. Mukherjee, T. Pham, K. A. Forrest, A. Kumar, B. Space, J. Kong, Q. Y. Zhang and M. J. Zaworotko, *Science*, 2019, **366**, 241–246.

3 Q. Ding, Z. Zhang, C. Yu, P. Zhang, J. Wang, X. Cui, C. H. He, S. Deng and H. Xing, *Sci. Adv.*, 2020, **6**, eaaz4322.

4 D. Lv, P. Zhou, J. Xu, S. Tu, F. Xu, J. Yan, H. Xi, W. Yuan, Q. Fu, X. Chen and Q. Xia, *Chem. Eng. J.*, 2022, **431**, 133208.

5 (*a*) Z. Zhang, L. Li, J.-X. Wang, H.-M. Wen, R. Krishna, H. Wu, W. Zhou, Z.-N. Chen, B. Li, G. Qian and B. Chen, *J. Am. Chem. Soc.*, 2020, **142**, 633–640; (*b*) H. Yang, Y. Wang, R. Krishna, X. Jia, Y. Wang, A. N. Hong, C. Dang, H. E. Castillo, X. H. Bu and P. Y. Feng, *J. Am. Chem. Soc.*, 2020, **142**, 2222–2227; (*c*) S.-M. Wang, X.-T. Mu, H.-R. Liu, S.-T. Zheng and Q.-Y. Yang, *Angew. Chem., Int. Ed.*, 2022, **61**, e202207066; (*d*) Y. Jiang, L. Wang, T. Yan, J. Hu, W. Sun, R. Krishna, D. Wang, Z. Gu, D. Liu, X. Cui, H. Xing and Y. Zhang, *Chem. Sci.*, 2023, **14**, 298–309; (*e*) Y. Jiang, J. Hu, L. Wang, W. Sun, N. Xu, R. Krishna, S. Duttwyler, X. Cui, H. Xing and Y. Zhang, *Angew. Chem., Int. Ed.*, 2022, **61**, e202200947; (*f*) Y. Gu, J.-J. Zheng, K. Otake, M. Shivanna, S. Sakaki, H. Yoshino, M. Ohba, S. Kawaguchi, Y. Wang, F. Li and S. Kitagawa, *Angew. Chem., Int. Ed.*, 2021, **60**, 11688–11694; (*g*) Y. Jiang, W. Yang, Y. Zhang, L. Wang and B. Chen, *J. Mater. Chem. A*, 2024, **12**, 5563–5580; (*h*) Y. Zhang, W. Sun, B. Luan, J. Li, D. Luo, Y. Jiang, L. Wang and B. Chen, *Angew. Chem., Int. Ed.*, 2023, **62**, e202309925.

6 (*a*) M. Ding, R. W. Flaig, H. L. Jiang and O. M. Yaghi, *Chem. Soc. Rev.*, 2019, **48**, 2783–2828; (*b*) K. Adil, Y. Belmabkhout, R. S. Pillai, A. Cadiau, P. M. Bhatt, A. H. Assen, G. Maurin and M. Eddaoudi, *Chem. Soc. Rev.*, 2017, **46**, 3402–3430; (*c*) L. Yang, S. Qian, X. Wang, X. Cui, B. Chen and H. Xing, *Chem. Soc. Rev.*, 2020, **49**, 5359–5406; (*d*) L. Yang, L. Yan, W. Niu, Y. Feng, Q. Fu, S. Zhang, Y. Zhang, L. Li, X. Gu, P. Dai, D. Liu, Q. Zhang and X. Zhao, *Angew. Chem., Int. Ed.*, 2022, **61**, e202204046; (*e*) L. Wang, N. Xu, Y. Hu, W. Sun, R. Krishna, J. Li, Y. Jiang, S. Duttwyler and Y. Zhang, *Nano Res.*, 2023, **16**, 3536–3541; (*f*) Z. Bao, J. Wang, Z. Zhang, H. Xing, Q. Yang, Y. Yang, H. Wu, R. Krishna, W. Zhou and B. Chen, *Angew. Chem., Int. Ed.*, 2018, **57**, 16020–16025; (*g*) Y. Jiang, Y. Hu, B. Luan, L. Wang, R. Krishna, H. Ni, X. Hu and Y. Zhang, *Nat. Commun.*, 2023, **14**, 401.

7 (*a*) E. D. Bloch, W. L. Queen, R. Krishna, J. M. Zadrozny, C. M. Brown and J. R. Long, *Science*, 2012, **335**, 1606–1610; (*b*) S. J. Geier, J. A. Mason, E. D. Bloch, W. L. Queen, M. R. Hudson, C. M. Brown and J. R. Long, *Chem. Sci.*, 2013, **4**, 2054–2061; (*c*) S. Yang, A. J. Ramirez-Cuesta, R. Newby, V. Garcia-Sakai, P. Manuel, S. K. Callear, S. I. Campbell, C. C. Tang and M. Schroder, *Nat. Chem.*, 2015, **7**, 121–129; (*d*) S. Tu, D. Lin, J. Huang, L. Yu, Z. Liu, Z. Li and Q. Xia, *Microporous Mesoporous Mater.*, 2023, **354**, 112532; (*e*) R.-B. Lin, L. Li, H.-L. Zhou, H. Wu, C. He, S. Li, R. Krishna, J. Li, W. Zhou and B. Chen, *Nat. Mater.*, 2018, **17**, 1128–1133.

8 (*a*) D. Lv, R. Shi, Y. Chen, Y. Wu, H. Wu, H. Xi, Q. Xia and Z. Li, *ACS Appl. Mater. Interfaces*, 2018, **10**, 8366–8373; (*b*) Y. Wang, S. Yuan, Z. Hu, T. Kundu, J. Zhang, S. B. Peh, Y. Cheng, J. Dong, D. Yuan, H.-C. Zhou and D. Zhao, *ACS Sustain. Chem. Eng.*, 2019, **7**, 7118–7126.

9 (*a*) X.-W. Gu, J. Pei, K. Shao, H.-M. Wen, B. Li and G. Qian, *ACS Appl. Mater. Interfaces*, 2021, **13**, 18792–18799; (*b*) R.-B. Lin, H. Wu, L. Li, X.-L. Tang, Z. Li, J. Gao, H. Cui, W. Zhou and B. Chen, *J. Am. Chem. Soc.*, 2018, **140**, 12940–12946.

10 Y. P. Li, Y. N. Zhao, S. N. Li, D. Q. Yuan, Y. C. Jiang, X. Bu, M. C. Hu and Q. G. Zhai, *Adv. Sci.*, 2021, **8**, 2003141.

11 (*a*) G.-D. Wang, K. Rajamani, Y.-Z. Li, W.-J. Shi, L. Hou, Y.-Y. Wang and Z. Zhu, *Angew. Chem., Int. Ed.*, 2022, **61**, e202213015; (*b*) G.-D. Wang, J. Chen, Y.-Z. Li, L. Hou, Y.-Y. Wang and Z. Zhu, *Chem. Eng. J.*, 2022, **433**, 133786; (*c*) Y. Ye, Y. Xie, Y. Shi, L. Gong, J. Phipps, A. M. Al-Enizi, A. Nafady, B. Chen and S. Ma, *Angew. Chem., Int. Ed.*, 2023, **62**, e202302564; (*d*) S.-Q. Yang, F.-Z. Sun, P. Liu, L. Li, R. Krishna, Y.-H. Zhang, Q. Li, L. Zhou and T.-L. Hu, *ACS Appl. Mater. Interfaces*, 2020, **13**, 962969; (*e*) X. Zhang, J. X. Wang, L. Li, J. Pei, R. Krishna, H. Wu, W. Zhou, G. Qian, B. Chen and B. Li, *Angew. Chem., Int. Ed.*, 2021, **133**, 10392–10398.

12 (*a*) L. Wang, W. Sun, Y. Zhang, N. Xu, R. Krishna, J. Hu, Y. Jiang, Y. He and H. Xing, *Angew. Chem., Int. Ed.*, 2021, **60**, 22865–22870; (*b*) W. Sun, J. Hu, S. Duttwyler, L. Wang, R. Krishna and Y. Zhang, *Sep. Purif. Technol.*, 2022, **283**, 120220; (*c*) Y. Zhang, J. Hu, R. Krishna, L. Wang, L. Yang, X. Cui, S. Duttwyler and H. Xing, *Angew. Chem., Int. Ed.*, 2020, **59**, 17664–17669; (*d*) Y. Zhang, L. Yang, L. Wang, X. Cui and H. Xing, *Angew. Chem., Int. Ed.*, 2019, **58**, 8145–8150; (*e*) Y. Zhang, L. Yang, L. Wang, X. Cui and H. Xing, *J. Mater. Chem. A*, 2019, **7**, 27560–27566; (*f*) Y. Zhang, L. Wang, J. Hu, X. Cui and H. Xing, *CrystEngComm*, 2020, **22**, 2649–2655; (*g*) W. Sun, Y. Jin, Y. Wu, W. Lou, Y. Yuan, S. Duttwyler, L. Wang and Y. Zhang, *Inorg. Chem. Front.*, 2022, **9**, 5140–5147; (*h*) L. Wang, W. Sun, S. Duttwyler and Y. Zhang, *J. Solid State Chem.*, 2021, **299**, 1221167.

13 (*a*) L. Gan, A. Chidambaram, P. G. Fonquernie, M. E. Light, D. Choquesillo-Lazarte, H. Huang, E. Solano, J. Fraile, C. Viñas, F. Teixidor, J. A. R. Navarro, K. C. Stylianou and J. G. Plansa, *J. Am. Chem. Soc.*, 2020, **142**, 8299–8311; (*b*) L. K. Macreadie, K. B. Idrees, C. S. Smoljan and O. K. Farha, *Angew. Chem., Int. Ed.*, 2023, **62**, e202304094; (*c*) K. B. Idrees, K. O. Kirlikovali, C. Setter, H. Xie, H. Brand, B. Lal, F. Sha, C. S. Smoljan, X. Wang, T. Islamoglu, L. K. Macreadie and O. K. Farha, *J. Am. Chem. Soc.*, 2023, **145**, 23433–23441; (*d*) Z. Li, D. Choquesillo-Lazarte, J. Fraile, C. Viñas, F. Teixidor and J. G. Planas, *Dalton Trans.*, 2022, **51**, 1137.

14 (*a*) X. Lian, P.-X. Liu, Y.-C. Yuan, J.-J. Pang, L. Li, S.-S. Liu, B. Yue, Y.-H. Zhang, L. Li, J. Xu and X.-H. Bu, *Adv. Funct. Mater.*, 2024, **34**, 2312150; (*b*) P. Zhang, L. Yang, X. Liu, J. Wang, X. Suo, L. Chen, X. Cui and H. Xing, *Nat. Commun.*, 2022, **13**, 4928.

15 L. Li, L. Guo, D. Olson, S. Xian, Z. Zhang, Q. Yang, K. Wu, Y. Yang, Z. Bao, Q. Ren and J. Li, *Science*, 2022, **377**, 335–339.

16 P.-Q. Liao, W.-X. Zhang, J.-P. Zhang and X.-M. Chen, *Nat. Commun.*, 2015, **6**, 8697.

17 J. Pires, J. Fernandes, K. Dedecker, J. R. B. Gomes, G. Pérez-Sánchez, F. Nouar, C. Serre and M. L. Pinto, *ACS Appl. Mater. Interfaces*, 2019, **11**, 27410–27421.

18 S. Geng, E. Lin, X. Li, W. Liu, T. Wang, Z. Wang, D. Sensharma, S. Darwish, Y. H. Andaloussi, T. Pham, P. Cheng, M. J. Zaworotko, Y. Chen and Z. Zhang, *J. Am. Chem. Soc.*, 2021, **143**, 8654–8660.

19 Z. Di, C. Liu, J. Pang, S. Zou, Z. Ji, F. Hu, C. Chen, D. Yuan, M. Hong and M. Wu, *Angew. Chem., Int. Ed.*, 2022, **61**, e202210343.

20 Y. Wang, C. Hao, W. Fan, M. Fu, X. Wang, Z. Wang, L. Zhu, Y. Li, X. Lu, F. Dai, Z. Kang, R. Wang, W. Guo, S. Hu and D. Sun, *Angew. Chem., Int. Ed.*, 2021, **60**, 11350–11358.

21 H.-G. Hao, Y.-F. Zhao, D.-M. Chen, J.-M. Yu, K. Tan, S. Ma, Y. Chabal, Z.-M. Zhang, J.-M. Dou, Z.-H. Xiao, G. Day, H.-C. Zhou and T.-B. Lu, *Angew. Chem., Int. Ed.*, 2018, **57**, 16067–16071.

22 C.-X. Chen, Z.-W. Wei, T. Pham, P. C. Lan, L. Zhang, K. A. Forrest, S. Chen, A. M. Al-Enizi, A. Nafady, C.-Y. Su and S. Ma, *Angew. Chem., Int. Ed.*, 2021, **60**, 9680–9685.

23 H. Zeng, X. J. Xie, M. Xie, Y. L. Huang, D. Luo, T. Wang, Y. Zhao, W. Lu and D. Li, *J. Am. Chem. Soc.*, 2019, **141**, 20390–20396.

24 Z. Xu, X. Xiong, J. Xiong, R. Krishna, L. Li, Y. Fan, F. Luo and B. Chen, *Nat. Commun.*, 2020, **11**, 3163.

25 Y. Liu, H. Xiong, J. Chen, S. Chen, Z. Zhou, Z. Zeng, S. Deng and J. Wang, *Chin. J. Chem. Eng.*, 2023, **59**, 9–15.

26 F. Xie, J. Liu, W. Graham, S. Ullah, E. M. C. Morales, K. Tan, T. Thonhauser, H. Wang and J. Li, *Chem. Eng. J.*, 2023, **473**, 145096.